Self-assembly and binding of a sorting nexin to sorting endosomes

Richard C. Kurten*, Anthony D. Eddington, Parag Chowdhury, Richard D. Smith, April D. Davidson and Brian B. Shank

Department of Physiology and Biophysics and Arkansas Cancer Research Center, University of Arkansas for Medical Sciences, 4301 West Markham Street, Little Rock, Arkansas 72205-0750, USA

*Author for correspondence (e-mail: KurtenRichardC@exchange.uams.edu)

Accepted 20 February 2001
Journal of Cell Science 114, 1743-1756 © The Company of Biologists Ltd

SUMMARY

The fate of endocytosed membrane proteins and luminal contents is determined by a materials processing system in sorting endosomes. Endosomal retention is a mechanism that traps specific proteins within this compartment, and thereby prevents their recycling. We report that a sorting nexin SNX1, a candidate endosomal retention protein, self-assembles in vitro and in vivo, and has this property in common with its yeast homologue Vps5p. A comparison of SNX1 expressed in bacterial and in mammalian systems and analyzed by size-exclusion chromatography indicates that in cytosol SNX1 tetramers are part of a larger complex with additional proteins. An endosomal retention function would require that SNX1 bind to endosomal membranes, yet the complexes that we analyzed were largely soluble and little SNX1 was found in pellet fractions. Using green fluorescent protein fusions, endocytic compartment markers and fluorescence recovery after photobleaching, we found that there is an equilibrium between free cytoplasmic and early/sorting endosome-bound pools of green fluorescent protein-SNX1. Fluorescence resonance energy transfer indicated that spectral variants of green fluorescent protein-SNX1 were oligomeric in vivo. In cell extracts, these green fluorescent protein-SNX1 oligomers corresponded to tetrameric and larger complexes of green fluorescent protein-SNX1. Using video microscopy, we observed small vesicle docking and tubule budding from large green fluorescent protein-SNX1 coated endosomes, which are features consistent with their role as sorting endosomes.

Movies available on-line:
http://www.biologists.com/JCS/movies/jcs2058.html

Key words: Intracellular membrane, Endosome, Sorting nexin 1, VPS10 protein, Green fluorescent protein

INTRODUCTION

Sorting decisions in the endosomal compartment determine the fate of cell surface receptors following endocytosis (Mukherjee et al., 1997). Endocytosed receptors enter the endo-lysosomal system where they may either be returned to the cell surface for reuse (recycling) or be transported to another compartment within the cell. Receptors for nutritional macromolecules are usually recycled (Davis et al., 1987; Dautry-Varsat et al., 1983), whereas receptors for hormones and growth factors are frequently degraded in lysosomal compartments (Felder et al., 1990; Herbst et al., 1994). Recycling appears to be by default and may rely on an iterative fractionation mechanism whereby endosomal membrane and membrane proteins are removed as tubules from sorting endosomes (Dunn et al., 1989). On excision from the sorting endosome, these tubules enter the recycling endosome compartment and eventually return to and fuse with the plasma membrane. Retention of growth factor receptors in sorting endosomes limits recycling and appears to require the recognition of specific traffic signals via protein-protein interactions (Herbst et al., 1994).

A candidate endosomal retention protein, sorting nexin 1 (SNX1), was identified in a yeast two-hybrid screen using the kinase domain of the EFG receptor. SNX1 binds to a region of the EGF receptor containing a lysosomal targeting code (Kurten et al., 1996). In overexpression experiments, SNX1 and the related proteins SNX2 and SNX4 coimmunoprecipitated with the EGF, insulin and PDGF receptor tyrosine kinases and also associated with transferrin receptors (Haft et al., 1998). SNX orthologs are widespread, having been identified in mice, flies worms and yeast. The yeast ortholog of SNX1, Vps5, has been shown genetically and biochemically to participate in trafficking of the carboxypeptidase Y receptor between the trans-Golgi network (TGN) and a prevacuolar compartment (Horazdovsky et al., 1997; Nothwehr and Hindes, 1997), suggesting a conservation of function for these proteins in intracellular membrane trafficking.

Epidermal growth factor receptors are preferentially endocytosed and degraded when bound by ligand (Honegger et al., 1987; Opresko et al., 1995). This downregulation is important for terminating signal transduction cascades that lead to cell proliferation (Vieira et al., 1996; Wells et al., 1990). Accelerated endocytosis may be mediated in part by the binding of AP-2 to EGF receptor residues 964-978 (Sorkin and Carpenter, 1993; Sorkin et al., 1996), and accelerated degradation by the binding of SNX1 to EGF receptor residues 954-958 (Kurten et al., 1996; Opresko et al., 1995). These two

trafficking signals are located in a region of the EGF receptor that is exposed following autophosphorylation-induced conformational changes in the receptor (Cadena et al., 1994; Nesterov et al., 1995a). Other regions and mechanisms are also involved in EGF receptor endocytosis (Chang et al., 1993) and lysosomal targeting (Opresko et al., 1995; Kornilova et al., 1996; Kil et al., 1999), such that no site single-handedly confers a particular property (Nesterov et al., 1995b). For example, ligand-activated EGF receptors can also recruit c-Cbl into endosomes, leading to receptor ubiquitination and subsequent lysosomal and proteosomal degradation (Levkowitz et al., 1998).

The EGF receptor sorting signal bound by SNX1 is similar to the tyrosine-based signal in the lysosomal membrane glycoproteins lamp-1 and lamp-2 that are primarily sorted at the TGN (Guarnieri et al., 1993). Recognition of the YxxΦ signal in TGN38 is via the μ1 subunit of the clathrin adaptor complex AP1 (Ohno et al., 1995), and leads to clathrin binding and vesicle budding at the TGN. Similarly, complexes of coat proteins facilitate budding from the endoplasmic reticulum (COP2; Aridor et al., 1998) and from the Golgi (Aoe et al., 1998; Goldberg, 2000). More recently, adaptor protein complexes AP3 (Faundez et al., 1998) and possibly AP4 (Goldberg, 2000) have also been identified as coat proteins. Coat protein assembly is specific and intimately related to the type of transport vesicle being formed. Thus, cargo selection and coat formation may be intimately linked. Endosomal retention may represent a refinement of coat protein function where the cargo selection mechanism is preferentially retained and not linked directly to vesicle budding.

In this study, we analyzed the oligomeric state of SNX1 and used the green fluorescent protein (GFP) (Chalfie et al., 1994; Presley et al., 1997) as a marker to examine the intracellular localization of SNX1 in living cells. We find that SNX1 self-assembles into a tetramer and that this complex binds tubular and vesicular endosomes that include some elements of the early endosome compartment. Using fluorescence recovery after photobleaching, we also document an exchange of subunits between soluble and membrane-bound pools of SNX1. The nature of the compartment labeled by GFP-SNX1, in particular our observation of tubule budding from larger GFP-SNX1 labeled vesicles, indicates a role for SNX1 in protein trafficking through the sorting endosome.

MATERIALS AND METHODS

Cell culture

Mammalian cells were cultured in DMEM/Ham's F-12 (50:50) supplemented with 15 mM Hepes, 2.5 mM L-glutamine, 5% calf serum and 100 i.u./ml penicillin, 100 μg/ml streptomycin, 0.25 μg/ml amphotericin B. HeLa cells expressing HA-tagged SNX1 were provided by Gordon Gill (University of California, San Diego, USA). African Green monkey kidney cells (CV1), human embryonic kidney cells (HEK 293) and human mammary tumor cells MCF7 were obtained from the American Type Culture Collection (Manassas, VA, USA), and the immortalized normal human mammary epithelial cell line (HB2; Berdichevsky et al., 1994) was provided by H. Steven Wiley, (Pacific Northwest National Laboratory, Richland, Washington, USA). CV1 transfections were performed with a total of 15 μg plasmid DNA in 6 cm diameter plastic dishes using the calcium phosphate precipitation method (Graham and Eb, 1973). Stably transfected cells were selected by trypsinization and dilution 48 hours post-transfection into medium containing 400 units/ml G418. Colonies were picked and maintained in 200 units/ml G418.

Preparation of mammalian cell extracts

Cells were rinsed with buffer (10 mM Hepes-KOH, pH 7.4 at 4°C, 10 mM KCl, 2 mM $MgCl_2$, 1 mM EDTA, 1 mM EGTA) and allowed to swell in the same buffer containing phosphatase and protease inhibitors (1 mM NaF, 10 mM benzamidine, 12.5 μg/ml aprotinin, 10 μg/ml leupeptin, 1 mM PMSF) for 10 minutes on ice. Buffer was decanted and residual buffer and cells were scraped and transferred to a 7 ml Dounce homogenizer (approx. 3 ml from six 15 cm dishes). Cells were homogenized with 20-30 strokes of a tight fitting pestle, diluted with an equal volume of 0.5 M sucrose, 10 mM Hepes-KOH, pH 7.4 at 4°C, 10 mM KCl, 1 mM EDTA, and homogenized with an additional 20 strokes using the tight pestle. Cell lysis was confirmed by phase-contrast microscopy. The homogenate was fractionated by differential centrifugation for 3 minutes at 5,380 ***g*** (P1), 10 minutes at 21,000 ***g*** (P2) and 30 minutes at 109,000 ***g*** (P3, pellet; S3, supernatant) using a Beckman TLA45 rotor.

Protein expression in bacteria

A GST-SNX1 expression plasmid was produced by cloning a 1.73 kb *Bam*HI/*Sal*I SNX1 fragment from pRCK5621 into *Bam*HI/*Xho*I digested pGEX-1NΔ. The resulting plasmid was digested with *Bam*HI, filled with Klenow, and religated in the presence of *Bam*HI to create an in-frame fusion of GST with SNX1 residues 77-522 (pRCK6156). pGEX-1NΔ was derived from pGEX1N (AMRAD Corporation Ltd., Kew, Victoria, Australia) by *Eco*RI digestion and insertion of a double-stranded, phosphorylated oligonucleotide formed by annealing 5′-aatttctcgagtcggccg-3′ and 5′-aattcggccgactcgaga-3′. For protein expression, 400 ml overnight cultures of BL21 cells transformed with pRCK6156 were diluted into 4L LB broth containing 1 ml 30% antifoam A emulsion (Sigma Chemical Company, St Louis, MO, USA) and aerated for 1 hour at room temperature. Protein expression was induced with 0.1 mM IPTG for an additional 6-10 hours. Cells were collected by centrifugation, washed with TBS (25 mM 2-amino 2-(hydroxymethyl)-1,3-propanediol, pH 7.4, 150 mM NaCl), resuspended in 100 ml buffer (1× TBS, 1% Triton X-100, 1 mM EDTA, 1 mM EGTA, 5 mM Benzamidine, 10 μg/ml Leupeptin, 1 mM PMSF) and 25 ml portions lysed by sonication with a probe-type sonicator (4×30 second bursts at 18 W using a 1/8″ probe). The lysate was clarified by centrifugation (20 minutes at 25,400 ***g*** in a Beckman JA20 rotor), allowed to stand on ice overnight and clarified a second time to remove the precipitate that formed. Portions of the lysate were incubated with glutathione-agarose and washed thoroughly with TBS.

For thrombin cleavage, 1 ml GST-SNX1 beads were washed 3 times with 10 ml TBS, 1% Triton X-100, twice with 10 ml TBS and once with 10 ml 2.5 mM $CaCl_2$ in TBS. The beads were resuspended with 1 ml 2.5 mM $CaCl_2$ in TBS and 4 NIH units of human thrombin (Sigma Chemical Co., St Louis, MO, USA) and incubated at room temperature for 2 hours. The beads were pelleted by centrifugation and the supernatant (containing cleaved SNX1) was collected. For chemical crosslinking, portions of the supernatant were crosslinked with freshly prepared Bis(sulfosuccinimidyl) suberate (BS3) (Pierce, Rockford, IL, USA) in a total volume of 30 μl over a range of concentrations for 30 minutes at 4°C. For analysis, samples were separated on 12% polyacrylamide gels and stained with Coomassie Blue.

GST-SNX1 binding assay

^{35}S-labeled SNX1 was produced using a coupled transcription-translation system (TNT, Promega Corp. Madison, WI, USA) and [^{35}S]methionine from Amersham (Arlington Heights, IL, USA). The template was a full-length SNX1 cDNA. In general, 10 μl of the translation mixture was added to 20 μg GST fusion protein

immobilized on glutathione-agarose in 200 μl reactions. Portions of the translation reactions were incubated with glutathione-agarose beads immobilized GST or GST-SNX1 for 1 hour at room temperature on a rotating wheel. After binding, the beads were washed with TBS and solubilized in SDS-sample buffer. Bound proteins were separated by SDS-PAGE and visualized by fluorography; the radioactive bands were excised and radioactivity quantified by liquid scintillation spectrometry.

GFP fusion proteins and expression

An *Eco*RI fragment containing the coding region of SNX1 was inserted into the vector pEGFP-C1 (CLONTECH Laboratories, Palo Alto, CA, USA) as follows. First, pEGFP-CI was modified by *Xho*I digestion, Klenow fill-in and religation to remove the *Xho*I site, thereby generating pEGFP-C1Δ*Xho*I. Next, SXN1 Expression plasmid pRCK5767 was digested with *Eco*RI and the *Eco*RI fragment was cloned into *Eco*RI cut, dephosphorylated pEGFP-C1Δ*Xho*I. The resulting EGFP-SNX1 plasmid (pRCK6255) contained the SNX1 cDNA encoding residues 1-522 in the proper orientation and was used in all transfection experiments. The resulting fusion proteins contained a 28 amino acid linker (SGLRSRSSSSFEFRDQFDLTVGITDPEK) between EGFP residue 239 and the initiator methionine of SNX1. pECFP-SNX1 and pEYFP-SNX1 were constructed by transferring a 2014 base pair *Bgl*II-*Sal*I SNX1 cDNA fragment from pRCK6255 into *Bgl*II-*Sal*I digested pECFP-C1 and pEYFP-C1.

SNX1 complex analysis by gel filtration

Soluble supernatant fractions (100 μl to 500 μl) were applied to a 1×30 cm Superdex 200 size-exclusion chromatography column in an FPLC® system (Pharmacia, Piscataway NJ, USA) operated at 4°C. The column was equilibrated and developed with TBS at a flow rate of 0.5 ml/minute. The column was calibrated by monitoring the ultraviolet absorbence of a set of globular proteins (cytochrome *c*, 12.4 kDa; carbonic anhydrase, 29 kDa; bovine serum albumin, 66 kDa; alcohol dehydrogenase, 150 kDa; β-amylase, 200 kDa; Blue Dextran, 2000 kDa) purchased from Sigma (St Louis, MO, USA). For immunoblot analysis, 1-ml fractions were collected, portions were separated by SDS-PAGE, and then transferred to polyvinylidene difluoride (PVDF) membranes (Millipore, Bedford, MA, USA) by electroblotting. The membranes were blocked with 5% Carnation® nonfat dry milk (Nestlé USA, Glendale, CA, USA) diluted in TTBS (0.1% poly(oxytheylene)n-sorbitan-monolaurate in TBS) and incubated with polyclonal anti-peptide antiserum specific for the carboxyl terminus of SNX1 (CYLEAFLPEAKAIS; Bethyl Labs, Montgomery, TX, USA) or the HA tag (CYPYDVPDYASL; Covance Inc., Princeton, NJ, USA) diluted in 1% Carnation® nonfat dry milk TTBS. Primary antibody binding was detected with alkaline phosphatase-conjugated affinity-purified goat anti-rabbit IgG (Fc) (Promega Corporation, Madison, WI, USA) followed by incubation with 0.4 mM NBT (nitrobluetetrazolium) and 0.45 mM BCIP (5-bromo-4-chloro-3-indolyl phosphate) in 100 mM Tris-HCl, pH 9.5, 100 mM NaCl, 5 mM $MgCl_2$. For analysis of intrinsic GFP fluorescence, 0.5 ml fractions were collected in 1 cm square methacrylate cuvettes, diluted with 0.5 ml TBS, and the fluorescence measured in a TD-700 fluorometer (Turner Designs, Sunnyvale, CA, USA) fitted with a 486 nm excitation filter and a 532 nm emission filter. The instrument was calibrated using TBS to set the photomultiplier tube offset and a 1:10 dilution of the loaded supernatant in TBS to set the gain.

Fluorescence microscopy

Epifluorescence microscopy of living cells was performed using a Zeiss Axiovert S inverted microscope fitted with a ×63, 1.4 numerical aperture PlanApo objective (Carl Zeiss, Inc. Thornwood, NY, USA), filter sets specific for GFP or Texas Red (#31001, #31004 Chroma Technology Corp., Brattleboro, VT, USA) and a 100 W mercury arc illuminator (Atto Instruments Inc, Rockville, MD, USA). Digital images were collected from the SCSI port of an 8-bit monochrome CCD camera (Hamamatsu C5985), using the vendor supplied application (HPS SCSI, Hamamatsu Photonic Systems, Bridgewater, NJ, USA). Color images were generated from pairs of monochrome images by psuedocoloring in Adobe Photoshop (San Jose, CA, USA) as follows. The image-adjust-auto levels function was applied to the red and green channels to normalize the intensity histograms, the colored images were overlayed using the difference mode, and the resulting image was exported as a TIF file. Minimal overlap was observed between the green and red channels at equivalent camera exposure settings.

Texas Red® labeled endocytic markers were purchased from Molecular Probes, Inc. (Eugene, OR, USA). For analysis of fluid-phase endocytosis, transiently transfected CV1 cells cultured on glass substrates were incubated with 0.5 mg/ml Texas Red Dextran (nominal molecular mass of 10,000 Da) diluted in 0.1% BSA, DMEM/Ham's F-12 (50:50), 15 mM Hepes, 2.5 mM L-glutamine for 1 hour at 37°C, rinsed in medium and immediately examined. For analysis of transferrin and EGF trafficking, CV1 cells were incubated with either 50 μg/ml transferrin-conjugated Texas Red® or 10 μg/ml biotinylated EGF conjugated to Texas Red®-streptavidin diluted in 0.1% BSA, DMEM/Ham's F-12 (50:50), 15 mM Hepes, 2.5 mM L-glutamine. The cells were incubated for 1 hour at 37°C prior to visualization. In a separate experiment, cells were labeled with Texas Red-EGF for 30 minutes at 4°C and then incubated for 30 minutes at 20°C. Following incubation, cells were washed in cold medium, fixed with 3.6% paraformaldehyde, 2.5 mM EDTA, 1 mM sodium vanadate in PBS, pH 7.2, for 15 minutes, rinsed with PBS and mounted in Prolong antifade compound (Molecular Probes, Inc, Eugene, OR, USA).

For indirect immunofluorescence, cells were cultured on coverslips and fixed in freshly prepared 3.6% paraformaldehyde, 0.24% saponin, 2.5 mM EDTA, 1 mM sodium vanadate in PBS, pH 7.2, for 15 minutes. Free aldehyde groups were reduced with 0.1% sodium borohydride in PBS for 10 minutes and cells were rinsed with PBS and incubated in buffer (20% goat serum, 1% BSA, 1 mM sodium vanadate in PBS, pH 7.2) for 20 minutes. Antibody binding and rinses were in the same buffer. Primary antibodies, dilutions and sources were as follows: affinity-purified rabbit polyclonal anti-SNX1 raised against the carboxyl-terminal peptide CYLEAFLPEAKAIS (1:200, Bethyl Labs, Montgomery, TX, USA); mouse monoclonal anti-EEA1 (1:300), mouse monoclonal anti-rab5 (1:100), mouse monoclonal anti-C-cbl (1:100), mouse monoclonal anti-TGN38 and mouse monoclonal anti-clathrin (1:100) were from Transduction Laboratories, Lexington, KY, USA. Mouse monoclonal anti-Lamp1 (H4A3; Chen et al., 1985) was from the Developmental Studies Hybridoma Database and was diluted 1:100. Secondary antibodies (Alexa 488-conjugated goat anti-rabbit immunoglobulin and Alexa 594-conjugated goat anti-mouse immunoglobulin; Molecular Probes, Eugene, OR, USA) were used at a 1:250 dilution. After washing, the preparations were mounted in Prolong antifade compound (Molecular Probes, Inc, Eugene, OR, USA) and viewed using a ×40, 1.3 numerical aperture Fluar objective fitted to a Zeiss LSM410 confocal microscope (Carl Zeiss, Inc., Thornwood NY, USA). The 488 nm and 568 nm lines of an argon-krypton laser were used for excitation and the red and green emissions were separated with a 580 nm dichroic beam splitter. A 590 nm longpass emission filter was used for the red channel and a 515-540 nm bandpass emission filter was used for the green channel. Images were collected as chunky RGB TIFF files. We did not detect substantial overlap between the red and the green channels. Colocalization was quantified by calculating the percentage overlap of GFP-SNX1 on the specific endosomal compartment being analyzed, using a custom macro in Scion Image (version Beta 3b, available at http://www.scioncorp.com/). Briefly, the green and red channels of the RGB image were converted into binary images, the binary images were multiplied to generate a binary overlap image, and the number of nonzero pixels in the overlap image divided by the

number of nonzero pixels in the GFP-SNX1 image calculated and converted to percentage overlap. Although only colocalized pixels will give a nonzero value in the product image, the selection of the threshold used to generate the binary images for calculating overlap has a significant influence on the result. We determined the appropriate threshold value of 150 (255 is black) by using a complete range (for 8-bit images, from 5 to 255 in steps of 5) of threshold values in test images.

CV1 cells cotransfected with EGF receptor-GFP (Carter and Sorkin, 1998) or GFP-rab5:Q79L (Roberts et al., 1999) and CFP-SNX1 were fixed with 0.9% paraformaldehyde in PBS, pH 7.2, for 15 minutes and were mounted in antifade compound (Prolong, Molecular Probes, Inc, Eugene, OR, USA). Cells were imaged by epifluorescence using a Zeiss Axiovert inverted microscope fitted with a 63×, 1.4 numerical aperture PlanApo objective and filter sets specific for GFP and CFP. Digital monochrome images for each channel were collected from the SCSI port of an 8-bit CCD camera (Hamamatsu C5985), using the vendor-supplied application (HPS SCSI, Hamamatsu Photonic Systems, Bridgewater, NJ, USA). In control experiments, no overlap was observed between the cyan and green channels at equivalent camera exposure settings.

For time-lapse studies, the camera video port was connected to a Scion LG-3 frame grabber card (Scion Corporation, Frederick MD, USA) and images stored as tagged image format (TIF) stacks using Scion Image. To minimize cell damage, the mercury arc illuminator was operated at reduced power and a neutral density filter was used to attenuate the incident radiation. These precautions permitted us to continuously image cells for at least 15 minutes without appreciable photobleaching or evidence of cell damage. Time-lapse images were collected over a period of 6-8 minutes.

For fluorescence photobleaching and recovery, fluorescence in a selected region was ablated using a 390 nm nitrogen-pumped BBQ dye laser (Cell Robotics Inc., Albuquerque, NM, USA) and a ×40, 1.3 numerical aperture Fluar objective. The laser power and duration used (10 pulses per second for 10 seconds) did not result in morphological responses within a 6 minute interval following the bleach. Nominal laser power output was 20 μJ/pulse, such that total irradiation was less than 2 mJ. Spot size was approx. 12 μm in diameter.

For analysis of fluorescence resonance energy transfer (FRET), we used a ×40, 1.3 numerical aperture Fluar objective (Carl Zeiss, Inc. Thornwood, NY, USA) and CYP/YFP FRET set XF89 from Omega Optical Inc. (Brattleboro, VT, USA). Excitation of CFP was with a 440±10.5 nm bandpass filter and dual emission images were collected using 480±15 nm and 535±13 nm bandpass filters (Miyawaki et al., 1997). Spatial averages of the fluorescence emission signals in individual cells were used to calculate an acceptor/donor ratio (spatially averaged emission ratio). If the fusion proteins are in close proximity to one another, the 480 nm emission from cyan fluorescent protein (CFP) (the donor) will excite fluorescence at 535 nm from yellow fluorescent protein (YFP) (the acceptor) (Wu and Brand, 1994). Although the emission spectrum of BFP shows much less overlap with its FRET partner GFP (Yang et al., 1998), the low quantum yield and rapid photobleaching of BFP precluded the use of BFP in our experiments. CFP/YFP alone provided a control for spectral overlap of the broad CFP emission spectrum with that for YFP emission and for excitation of YFP with the 440 nm filter (Pollok and Heim, 1999).

Online supplemental materials

QuickTime movies were made using Adobe Premier (version 4.2). Images were first collected using a Scion LG-3 frame grabber card (Scion Corporation, Frederick MD, USA) and stored as a tagged image format (TIF) stack using Scion Image (version Beta 3b, available at http://www.scioncorp.com/). The TIF stack was converted to a TIF sequence using a Scion Image macro and the files imported into Adobe Premier. When required, the brightness and contrast of the last frame was matched to the first frame of the movie clip using a filter function and the filter progressively applied from the beginning to the end. QuickTime movie was output at 320 (horizontal) × 240 (vertical) at 15 frames per second using a compression ratio of 43%.

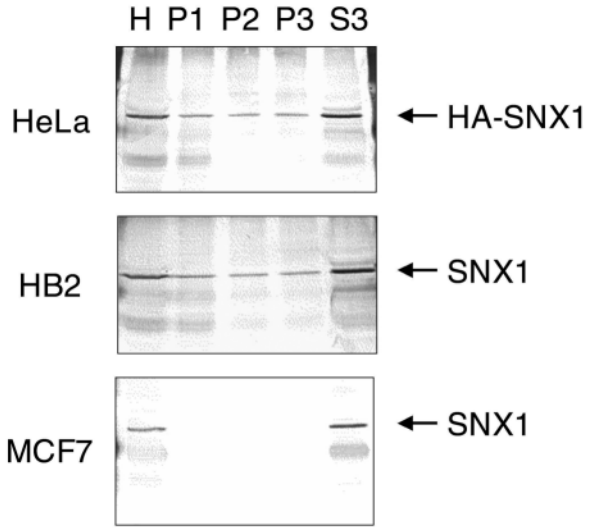

Fig. 1. SNX1 is largely soluble in subcellular fractions. Cultured cells were broken open by Dounce homogenization in low ionic strength buffer. The homogenate was adjusted to 0.25 M sucrose (H) and fractionated by differential centrifugation to generate P1 (1.6×10^4 $\boldsymbol{g}_{min}$), P2 (2.2×10^5 $\boldsymbol{g}_{min}$) and P3 (3.3×10^6 $\boldsymbol{g}_{min}$) pellet fractions and a cytosolic fraction (S3, 3.3×10^6 $\boldsymbol{g}_{min}$ supernatant). Equivalent proportions of each fraction were analyzed by western blotting using an affinity-purified polyclonal antibody specific for the carboxyl terminus of SNX1. For HeLa cells, transfected HA-tagged SNX1 was analyzed. For HB2 and MCF7 cells, endogenous SNX1 was analyzed.

RESULTS

Cytosolic SNX1 is oligomeric

The subcellular distribution and oligomerization of SNX1 in extracts from mammalian cells was examined in HeLa cells that were engineered to overexpress an influenza hemaglutinin epitope-tagged SNX1 (HA-SNX1). Subcellular fractions were prepared by differential centrifugation of low ionic strength homogenates and analyzed by western blotting with an antibody specific for SNX1. Under these conditions, the majority of HA-SNX1 was found in the cytosolic fraction, with a small proportion in membrane fractions (Fig. 1). Similarly, endogenous SNX1 in immortalized human mammary epithelial cells (HB2) and in human mammary carcinoma cell (MCF7) extracts was largely soluble under these same conditions. To determine the oligomerization status of soluble HA-SNX1 in mammalian cells, HeLa cytosol proteins were separated by size-exclusion chromatography and fractions analyzed by western blotting using an anti-HA antibody (Fig. 2A). HA-SNX1 eluted over several fractions with the peak in a fraction that corresponded to a tetramer of SNX1 (the calculated molecular mass of a tetramer is 237 kDa). The peak was not symmetrical and was skewed toward the void volume, suggesting that substantial amounts of SNX1 are also in larger complexes. No SNX1 was detected in fractions that would correspond to monomers. We also produced [^{35}S]methionine-

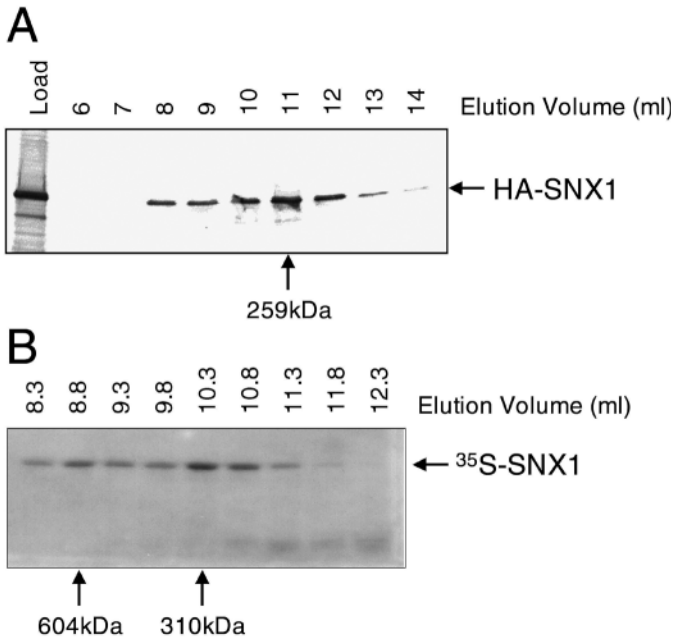

Fig. 2. Recombinant SNX1 forms tetrameric and larger complexes in eukaryotic cytosols. (A) Hela cell cytosol (LOAD) containing HA-SNX1 was applied to a Superdex 200 size exclusion column and eluted in 1 ml fractions that were monitored by western blotting using an HA-specific antibody. The vertical arrow indicates the molecular mass in the middle of the peak fraction based on comparison with a series of globular standards. The calculated molecular mass of the SNX1 tetramer is 237 kDa. (B) Full-length [^{35}S]methionine-labeled SNX1 was translated in vitro in a reticulocyte lysate and the reaction mixture applied to a Superdex 200 gel filtration column. Fractions (0.5ml) were collected and analyzed for SNX1 by SDS-PAGE and fluorography. The vertical arrows indicate the molecular mass in the middle of the two peak fractions based on comparison with a series of globular standards.

labeled SNX1 (residues 1-522) by in vitro translation in a reticulocyte lysate and separated the reaction by size-exclusion chromatography. The chromatographic behavior of ^{35}S-SNX1 was analyzed by SDS-PAGE and fluorography to detect the radiolabeled protein (Fig. 2B). As observed for HA-SNX1 from HeLa cell extracts, ^{35}S-SNX1 produced in vitro in a reticulocyte lysate also eluted in fractions of a size corresponding to a prominent tetrameric complex, as well as larger complexes of SNX1. The prominent tetrameric species for both HA-SNX1 from HeLa cytosol and ^{35}S-SNX1 translated in vitro indicates that oligomerization is an intrinsic property of the protein.

In HeLa cell lysates and in the reticulocyte lysate, the binding of other proteins rather than oligomerization of SNX1 could account for the large size of the SNX1 complex. To more rigorously define the intrinsic oligomerization properties of SNX1, a fusion protein between glutathione S-transferase and SNX1 (residues 77-522, SNX1$_{77\text{-}522}$) was expressed in bacteria and purified on glutathione-Sepharose beads. To determine if SNX1 was capable of oligomerization, GST-SNX1$_{77\text{-}522}$ immobilized on glutathione-Sepharose beads was incubated with [^{35}S]methionine-labeled SNX1 (residues 1-522) produced by in vitro translation in a reticulocyte lysate reaction. After washing, the bead-bound radioactivity was extracted and analyzed by SDS-PAGE and fluorography (Fig. 3A). Immobilized GST-SNX1$_{77\text{-}522}$ bound a large fraction of added ^{35}S-SNX1 (Fig. 3A, GST-SNX1 + Probe). By contrast, immobilized GST bound less than 10% of the input radioactivity (Fig. 3A, GST + Probe, compare to 10% Probe). This indicates that SNX1 is at least capable of dimerization and that dimerization is specific. To determine the nature of the oligomer in solution, SNX1$_{77\text{-}522}$ was cleaved from immobilized GST-SNX1$_{77\text{-}522}$ with thrombin and chemically crosslinked with BIS-(sulfosuccinimidyl) suberate (BS3) (Fig. 3B). Whereas the cleaved protein migrated as a monomer in reducing SDS-PAGE gels stained with Coomassie Blue, the crosslinked protein was converted into oligomers, including species consistent with dimers and tetramers. However, the crosslinks did not appear to represent a quantitative conversion of monomers into dimers and tetramers, even when the gels were transferred and analyzed by immunoblotting using antibodies specific for SNX1 (data not shown). Therefore, we chromatographed cleaved SNX1$_{77\text{-}522}$ (without crosslinking) on a size-exclusion column to determine the nature of the complex (Fig. 3C,D). When analyzed under native conditions, SNX1$_{77\text{-}522}$ chromatographed as a symmetrical peak that corresponded exactly to a tetramer (Fig. 3C). Crosslinking was not required, indicating that the tetramer is a stable species in solution. To assess complex stability, the fractionation was repeated in the presence of 6 M urea (Fig. 3D). Under these conditions, the tetramer was dissociated into a mixture of mostly dimeric SNX1 with a small proportion of monomer. These results indicate that the preferred oligomer of SNX1$_{77\text{-}522}$ is a tetramer and that the assembly of this tetramer probably proceeds through a dimeric intermediate. Whereas bacterial SNX1$_{77\text{-}522}$ yielded no complex larger than a tetramer (Fig. 3C), both HA-SXN1 (Fig. 2A) and ^{35}S-SNX1 (Fig. 2B) did, indicating that SNX1 tetramers in mammalian cell extracts may bind additional cytosolic proteins not present in bacterial extracts.

GFP-SNX1 binds endosomal membranes in mammalian cells

By contrast with the solubility of SNX1 in cell extracts, indirect immunofluorescence experiments indicate that SNX1 is associated with endosomal membranes in CV1 cells (Kurten et al., 1996). To examine this apparent discrepancy, we tagged SNX1 with GFP at its amino terminus (GFP-SNX1) and examined its localization in living cells using epifluorescence microscopy. We focussed on CV1 cells because they are flat and therefore well-suited to epifluorescence imaging at low illumination intensities, permitting high-resolution time-lapse imaging without coincident radiation damage. Following transient transfection of this cDNA into a variety of cell lines (CV1, HEK 293, MCF7, HB2), we found GFP-SNX1 localized to tubular and vesicular structures inside cells (Fig. 4A). Frequently, tubules extending over 10 or more μm appeared to either fuse with or bud from some of the larger vesicles. In addition to membrane localization, substantial cytoplasmic fluorescence was also easily detectable in all GFP-SNX1 transfected cell lines, consistent with the presence of the soluble pool in cell extracts (Fig. 1). GFP-SNX1 was stable for at least 96 hours in transiently transfected cells and was not toxic. However, GFP-SNX1 expression was severely attenuated in stable CV1 cell lines selected with the antibiotic

G418. Within the GFP-SNX1 colonies, less than 10% of the cells exhibited green fluorescence. These cells were never clustered in such a way that would indicate colonies of subpopulations of cells in the culture, leading us to hypothesize that expression of the GFP-SNX1 was growth inhibitory such that transgene was repressed. By contrast to the apparent repression of GFP-SXN1 in stable CV1 cell lines, the expression of GFP was uniform. GFP-SNX1 expression could be partially restored in stable CV1 cell lines by treatment with 2 mM sodium butyrate, a histone deacetylase inhibitor (Candido et al., 1978; Sealy and Chalkley, 1978), which can reverse repression of some genes (Milsted et al., 1987), for 48-72 hours. There was a dramatic increase in the number of GFP-SNX1 expressing cells following sodium butyrate treatment (data not shown), which corresponded to an increase in the total mass of GFP-SNX1 as assessed by western blotting of cell extracts (Fig. 4B). Thus, SNX1 expression is subject to repression in stable CV1 cell lines. Coincident with the derepression of GFP-SNX1 expression by sodium butyrate treatment, there was also a decrease in EGF receptor mass in the same extracts (Fig. 4B). In control experiments using stable GFP expressing CV1 cell lines, sodium butyrate also caused a decrease in EGF receptor mass such that the overall effect of GFP-SNX1 was an approximately 20% reduction in EGF receptor mass in the population (data not shown). By contrast, overexpression of GFP-SNX1 did not appear to be growth inhibitory in HEK 293 cells and GFP-SNX1 expression was not attenuated in stable transfectants (data not shown). Our HEK 293 cells and those of others (Slaaby et al., 1998) express low levels of EGF receptors, indicating that the growth inhibition by GFP-SNX1 in CV1 cells may be EGF-receptor-specific. Taken together, these results indicate that GFP-SNX1 has functional properties similar to wild-type SNX1. We also generated BFP, CFP and YFP fusions to the amino terminus of SNX1 and found that their distribution in transiently transfected CV1 cells was identical to that for GFP-SNX1 (data not shown). Cells transfected with CFP, GFP or YFP fusions alone showed diffuse cytoplasmic and nuclear fluorescence (Fig. 4C).

To determine if the vesicular compartment labeled by GFP-SNX1 was an endocytic compartment, GFP-SNX1 transfected cells were labeled Texas Red-labeled fluid phase markers at 37°C to determine if they would enter GFP-SNX1 labeled tubules and vesicles. To trace fluid-phase endocytosis, cells

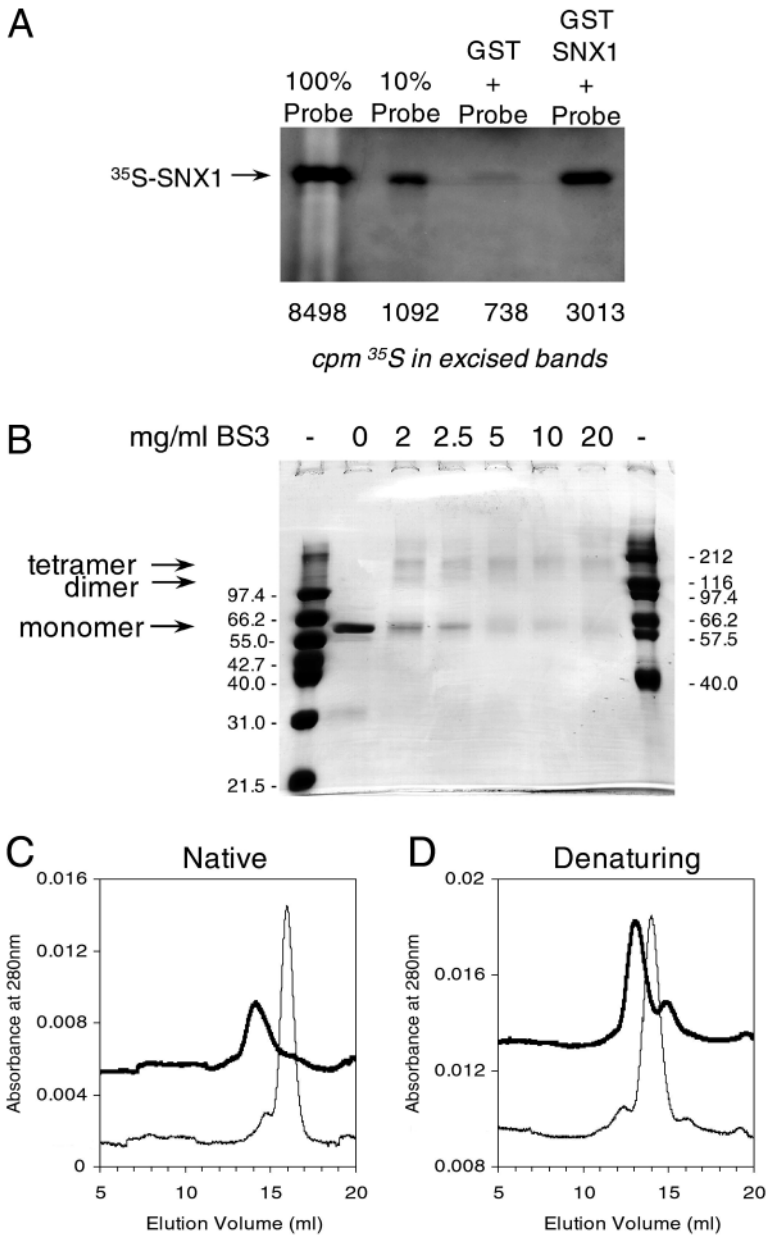

Fig. 3. SNX1 produced in bacteria self-assembles into tetramers. (A) [^{35}S]methionine-labeled SNX1 (Probe) was produced by in vitro translation using a reticulocyte lysate. GST and GST-SNX1 were expressed in bacteria, immobilized on glutathione-Sepharose beads, and incubated with ^{35}S-SNX1 probe at room temperature for 30 minutes. The total amount of radioactivity added to the binding reactions is indicated in the lane labeled 100% Probe. For comparison, a second lane was loaded with 1/10th volume of binding reaction mixture (10% Probe). After incubation, the beads were washed twice with Tris-buffered saline, extracted with SDS, and bound radioactivity visualized by SDS-PAGE and fluorography. Radioactivity was quantified by liquid scintillation spectrometry of the excised bands. (B) Bacterial GST-SNX1 was eluted from glutathione-agarose beads by cleavage with thrombin to yield a truncated SNX1 protein (residues 77-521, calculated molecular mass 51.7 kDa). Identical sample sizes of the eluted protein were incubated with the indicated concentrations of crosslinker and analyzed by SDS-PAGE and Coomassie Blue staining. The relative molecular masses (in kDa) of standards are indicated. (C,D) Bacterial SNX1$_{77\text{-}521}$ was applied to a Superdex 200 gel filtration column and elution monitored by ultraviolet absorbence at 280 nm. The column was equilibrated with Tris-buffered saline (C) or with 6 M urea in Tris-buffered saline (D). For size comparison, the elution of BSA (66 kDa) under identical conditions is also plotted in the thinner tracing in each chromatogram. The thicker SNX1$_{77\text{-}521}$ tracings are offset for clarity. BSA chromatographed as a prominent 66 kDa monomer peak with a small dimer peak (132 kDa). SNX1$_{77\text{-}521}$ tetramers (207 kDa) eluted prior to the BSA dimer, SNX1$_{77\text{-}521}$ dimers (103 kDa) eluted between the BSA dimer and monomer, and SNX1$_{77\text{-}521}$monomers (51.7 kDa) eluted after the BSA monomer. SNX1 monomers were detectable only after urea denaturation.

were incubated with Texas Red-dextran for 1 hour at 37°C and examined by epifluorescence microscopy. The lumens of some (but not all) of the larger vesicles were labeled with Texas Red-dextran (Fig. 4D), indicating that the compartment labeled by GFP-SNX1 was endocytic. To identify the recycling endosome compartment, cells were labeled to steady state for 1 hour at 37°C with Texas Red-transferrin (Fig. 4E). Under these conditions, GFP-SNX1 and transferrin labeled vesicles were largely distinct from one another. Apparent colocalization of GFP-SNX1 and transferrin labeled vesicles was limited to the perinuclear region. However, even in this region there were numerous distinct GFP-SNX1 and Texas Red transferrin labeled vesicles. Late endosomes and lysosomes were identified by labeling to steady state for 1 hour at 37°C with Texas Red-EGF (Fig. 4F). As was the case for transferrin, GFP-SNX1 and EGF labeled vesicles were largely distinct with colocalization of GFP-SNX1 and EGF labeled vesicles limited to the perinuclear region. However, even in this region there were numerous distinct Texas Red filled and GFP-SNX1 labeled vesicles. Pulse-chase experiments using Texas Red-EGF were complicated by fluorophore bleaching and low levels of endogenous EGF receptors in GFP-SNX1 expressing cells. However, by fixing the cells and mounting in antifade compound, the red fluorescence was better preserved. When cells were labeled with Texas Red-EGF at 4°C and incubated for an additional 30 minutes at 20°C, there appeared to be considerable overlap between the GFP-SNX1 and EGF-positive compartments (Fig. 4G). Despite the overlap, there remained numerous distinct green and red vesicles (Fig. 4H), and we did not detect any clear examples of GFP-SNX1 labeled vesicles that contained EGF as was the case for Texas Red-dextran (Fig. 4D). This may be due to a loss of tubule preservation during fixation. The steady-state labeling experiments allow us to reliably conclude that GFP-SNX1 does not overlap substantially with recycling endosomes, late endosomes, or lysosomes. In addition, the staining observed following incubation with Texas Red-EGF at 20°C indicates that the endosomal compartment labeled by GFP-SNX1 might include early and/or sorting endosomes.

To more precisely define the endosomal compartment labeled by GFP-SNX1, we used a panel of antibodies in a series of colocalization experiments (Fig. 5). GFP-SNX1 was visualized by intrinsic fluorescence as well as by staining with a rabbit polyclonal anti-SNX1 antibody, and the other compartments were visualized with mouse monoclonal antibodies. Percentage colocalization was calculated in paired digital images generated by confocal microscopy by measuring the percentage of all SNX1-positive pixels that were also positive for the second marker in the analysis. There was substantial, but not complete, colocalization of GFP-SNX1 with EEA1 (55% n=14 cells; Fig. 5A), C-cbl (27%, n=8 cells; Fig. 5B) and clathrin (36%, n=10 cells; data not shown). There was less colocalization with the trans-Golgi network marker TGN38 (14%, n=7 cells; Fig. 5C) and with late endosomes and lysosomes using anti-LAMP1 (20%, n=8 cells; Fig. 5D). Thus, GFP-SNX1 is partially localized to the early endosomal compartment and with a component of the ubiquitin ligation machinery (Levkowitz et al., 1999) implicated in proteolytic processing of EGF receptor in early endosomes (Levkowitz et al., 1998). We also attempted to colocalize SNX1 to the early endosomal compartment with rab5 antibodies but the endogenous rab5 signals were consistently weak. As an alternative approach to visualizing endogenous rab5 with antibodies, we contransfected cells with GFP-rab5 (Roberts et al., 1999) and CFP-SNX1 and were able to detect colocalization (data not shown). More striking was the colocalization of GFP-SNX1 with GFP-rab5:Q79L, a GTPase-deficient mutant mimicking the active GTP-bound conformation of rab5 that leads to enlargement of the early endosomal compartment. Both CFP-SNX1 and GFP-rab5:Q79L were on the same enlarged vesicles (Fig. 6A,B). However, CFP-SNX1 tubules were not equivalently labeled with GFP-rab5:Q79L (Fig. 6A,B inserts), suggesting that the tubules represent a compartment distinct from early endosomes.

To better examine the relationship between EGF receptor trafficking and the GFP-SNX1 labeled endosomes than was possible with Texas Red-EGF, CV1 cells were cotransfected with a GFP-tagged EGF receptor and CFP-SNX1. The GFP-tagged EGF receptor has been shown to have trafficking and signaling characteristics nearly identical to wild-type EGF receptors (Carter and Sorkin, 1998). In cells cultured in the presence of serum, there was colocalization of internalized EGF receptor-GFP with GFP-SNX1 (Fig. 6C,D). By contrast to GFP-rab5:Q79L, where there was no labeling on tubules (Fig. 6A,B, inserts), there was detectable EGF receptor-GFP in the CFP-SNX1 labeled tubules (Fig. 6C,D, inserts). Colocalization in tubules was most apparent in cells cultured in serum, where low levels of EGF induce steady-state trafficking of EGF receptors. We also treated cells with EGF after serum starvation with similar results, except that the expected internalization of receptors was accompanied by membrane ruffling and filapodial contractions that precluded epifluorescence imaging of tubules (data not shown).

To determine the relationship between GFP-SNX1 tubules containing EGF receptor-GFP and vesicles containing both GFP-SNX1 and rab5, we examined living GFP-SNX1-expressing cells by time-lapse video microscopy. We detected numerous instances of tubular endosomes associated with large GFP-SNX1 labeled vesicles (compare Figs 4A, 6B,D with Fig. 7A). When these vesicular and tubular complexes were viewed over time, we found that the tubules were derived from the large vesicles in a budding process that lasted for several minutes (Fig. 7A, movie 1). The tubules moved toward the periphery of the cell as well as toward the perinuclear region and consistently originated in locations distinct from the perinuclear concentrations of GFP-SNX1 fluorescence. Although we observed docking of small and large vesicles, we never observed the docking or fusion of tubules with any of the large vesicles. Vesiculo-tubular structures are frequently found in living cells, but they are not always detectable and may therefore represent transient entities. We have observed one instance in which a tubulo-vesicular structure enlarges and is depleted by tubules within a few minutes (Fig. 7B, movie 2). These observations indicate that there is vectorial membrane transport out of GFP-SNX1 labeled vesicles via tubular intermediates. Taken together, these compartment-marker and time-lapse studies indicate that GFP-SNX1 binds to a structure with characteristics that have been ascribed to sorting endosomes (Mukherjee et al., 1997).

The association of GFP-SNX1 with endosomes in living

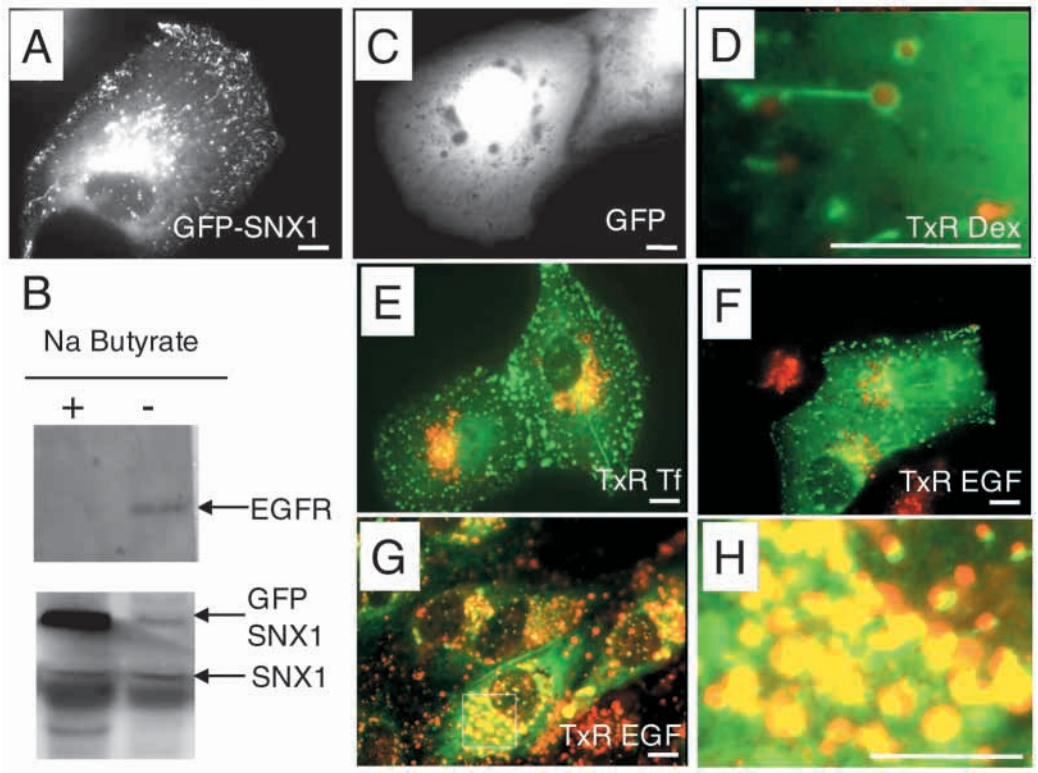

Fig. 4. GFP-SNX1 localizes to endosomal tubules and vesicles in living cells. CV1 cells were transfected with GFP-SNX1 (A) or with GFP (C) and the localization of green fluorescence was analyzed by epifluorescence microscopy. (B) Extracts from a clonal line of stably transfected cells cultured in the presence (+) or absence (–) of 2 mM sodium butyrate for 48 hours were assayed for expression of the proper fusion protein by western blotting using an antibody specific to the carboxyl terminus of SNX1. In the same lysates, the steady-state levels of EGF receptors (EGFR) were also examined. (D) In living cells, the lumen of the compartment labeled by GFP-SNX1 (green) was accessible to Texas Red dextran during a 1 hour incubation at 37°C (red). (E,F) There was little colocalization of GFP-SNX1 (green) with the Texas Red-transferrin labeled recycling endosome compartment (red) (E) or with the Texas Red-EGF labeled late endosomes or lysosomes (red) (F), as defined by steady-state tracer distribution in cells incubated with the tracer for 1 hour at 37°C. (G,H) By contrast, there was more apparent overlap between GFP-SNX1 and Texas Red EGF when the cells were labeled for 30 minutes at 4°C and incubated for 30 minutes at 20°C (G). (H) An enlargement of the boxed area in G that shows the close proximity of GFP-SNX1 (green) and EGF labeled vesicles (red). Scale bars, 10 μm.

cells, the easily detectable cytoplasmic pool of SNX1 and the solubility of endogenous SNX1 and GFP-SNX1 in low ionic strength extracts (Fig. 1) indicate that SNX1 is probably weakly bound to membranes. The fact that both SNX1 and GFP-SNX1 are membrane associated, as judged by light microscopy, could indicate that the membrane-bound and soluble pools of SNX1 are in equilibrium. To test this hypothesis, vesicular GFP-SNX1 fluorescence in living cells was bleached with a laser and fluorescence recovery was monitored (Fig. 8A, movie 3). Rapid recovery of cytoplasmic fluorescence ($t_{1/2}$=10.5±0.5 seconds) was followed by slower recovery of vesicular fluorescence ($t_{1/2}$=14.0±0.6 seconds, P<0.001) (Fig. 8B). The laser photobleaching did not damage the cells (as judged by a lack of membrane retraction around the periphery of the cell) nor did it abolish motility of labeled vesicles through the bleached zone. Thus GFP-SNX1, and by inference, SNX1, rapidly exchanges between membrane-bound and cytoplasmic pools.

GFP-SNX1 is oligomeric in vivo

Our biochemical results provide evidence that SNX1 is a stable tetramer that may be complexed with other proteins in cytosolic extracts of mammalian cells. To determine if SNX1 was similarly homo-oligomeric in living cells, we measured fluorescence resonance energy transfer (FRET) between modified green fluorescent proteins used to tag SNX1 proteins. CV1 cells were cotransfected with equimolar amounts of plasmids encoding CFP-SNX1 and YFP-SNX1. Spatially averaged emission ratios for individual cells were calculated from images generated by excitation at 440 nm and emission at 480 nm and at 535 nm. The spatially averaged emission ratio for the SNX1-CFP/SNX1-YFP pair was significantly higher (P<0.001) than the emission ratio for CFP/YFP (Fig. 8C) and for SNX1-CFP or SNX1-YFP alone (data not shown). Thus, in living cells, GFP variant-tagged SNX1 exists in a homo-oligomeric complex. The complex probably consists of a core tetramer (Figs 2, 3). This was examined by chromatography of cytosolic extracts prepared from cells expressing GFP-SNX1. To improve resolution, smaller fractions were collected than in previous experiments and GFP-SNX1 was detected by measuring green fluorescence using a filter fluorometer. At least two species of GFP-SNX1 were evident: a shoulder of green fluorescence corresponding to tetrameric SNX1, in addition to a stronger peak of green fluorescence corresponding to a 565 kDa complex (Fig. 8D). By contrast, GFP chromatographed as a 27 kDa monomer (data not shown). No

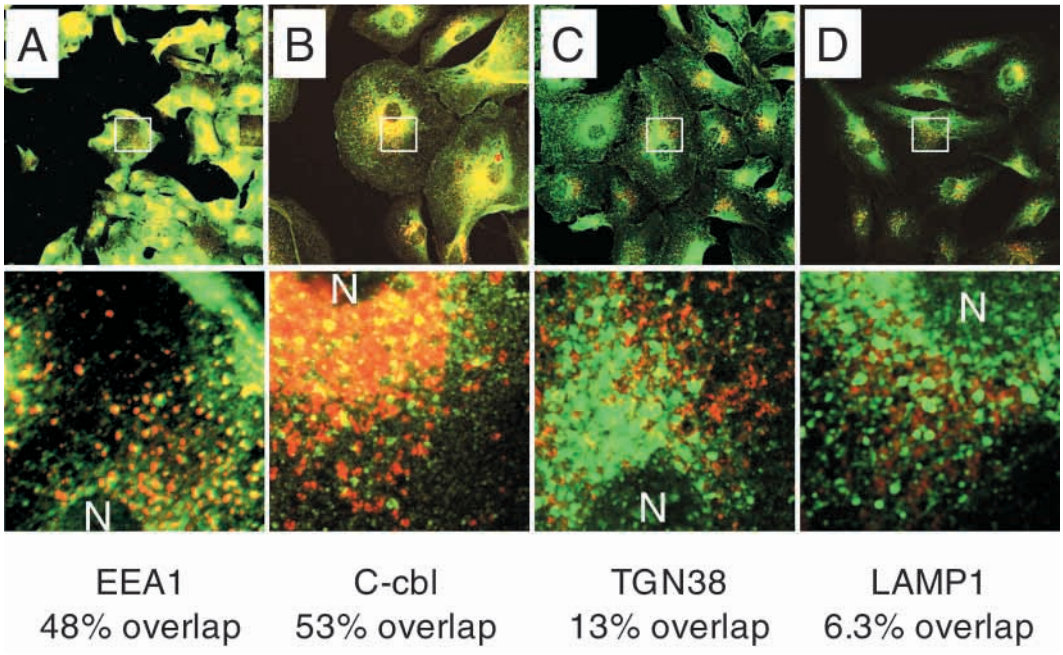

Fig. 5. Colocalization analysis of GFP-SNX1 coated endosomes. Stably transfected CV1 cells expressing GFP-SNX1 were fixed and stained with monoclonal antibodies (red) against EEA1 (A), C-cbl (B), TGN38 (C) and LAMP1 (D) in combination with a polyclonal antibody specific for SNX1 (green). The overall distribution of the proteins in the cells was visualized by confocal microscopy using a ×40 objective and with dual-label excitation and imaging. Colocalization was analyzed in images of the perinuclear compartment collected using the 8×-zoom function of the microscope (lower panels, 31 μm×31 μm). The percentage of the GFP-SNX1 compartment that was colocalized with the indicated compartment marker (pixel value <150 in both the red and the green channels) in the zoomed areas are listed below each column. The average percentage colocalization measured from 7-14 cells per marker is listed in the text.

fluorescence corresponding to GFP or to GFP-SNX1 monomers and dimers was detected in the GFP-SNX1 cytosols.

DISCUSSION

SNX oligomers are tetrameric

These studies establish SNX1 as a component of a large complex in extracts that reversibly associate with membranes of the endosomal compartment in living cells. The complex appears to be composed in part of SNX1 tetramers. Purified, bacterially expressed SNX1 was tetrameric in gel filtration and chemical cross-linking experiments. Similarly, soluble SNX1 translated in vitro, HA-SNX1 expressed in HeLa cells, or GFP-SNX1 expressed in HEK293 cells also behaved as a tetramer during size-exclusion chromatography. In addition, larger complexes were also detected in each sample that probably result from the binding of additional soluble proteins present in cytosols (Haft et al., 2000; Chin et al., 2000). These proteins appear to be limiting in overexpression experiments leading to the formation of at least two complexes, a tetrameric complex containing only SNX1 and a second complex containing SNX1 and associated proteins. This behavior is most apparent in experiments with GFP-SNX1, where we improved the resolution of our size-exclusion chromatography analysis by measuring green fluorescence in chromatographic fractions rather than using immunoblot analysis. By FRET analysis, we confirm that SNX1 is indeed homo-oligomeric in living cells. However, the FRET experiments cannot define the number of SNX1 monomers present in the complex. Although the tetramer behaves as a stable species in solution, the ability of ^{35}S-SNX1 to bind to immobilized SNX1 indicates that it is possible to exchange subunits between tetramer. When treated with urea, the SNX1 tetramer dissociates into dimers and monomers with the dimeric species predominating, indicating that the dimer is stable and is an intermediate in the formation of tetramers and perhaps additional complexes. This is likely to be important in the formation of heterotetrameric complexes between SNX1 and the closely related protein SNX2, which has been shown to coimmunoprecipitate with SNX1 (Haft et al., 1998), or in the formation of SNX complexes with other proteins. Thus, we propose that the fundamental unit of exchange between complexes is the homodimer.

Yeast Vps5p is homologous to SNX1 (Horazdovsky et al., 1997; Nothwehr and Hindes, 1997). Vps5p participates in CpY receptor trafficking and, like SNX1, is capable of self-assembly. Four additional proteins have also been identified in a large complex with Vps5p: Vps35p, Vps29p, Vps26p and Vps17p (Seaman et al., 1998). This complex, termed retromer, is proposed to provide a coat function for retrograde trafficking of Vps10p. Human orthologs for three of these proteins have been identified and found to exist in a complex with SNX1 under certain conditions (Haft et al., 2000). However, these complexes, which are proposed to contain hVps35 as their core, do not appear to be large enough to contain SNX tetramers. In cotransfection experiments, complexes between SNX1 and the human retromer components required simultaneous expression of SNX1, hVps35, hVps29 and hVps26, which led to the apparent disruption of a larger SNX1 complex. Thus, it is possible that SNX1 is a component of

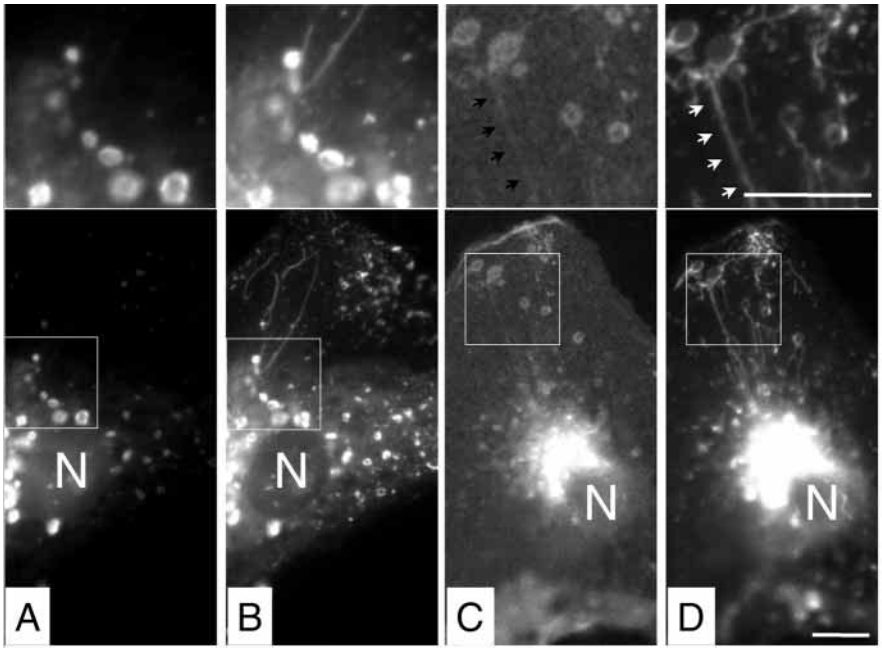

Fig. 6. Colocalization of GFP-rab5:Q79L and EGF receptor-GFP with CFP SNX1. CV1 cells were transiently cotransfected with CFP-SNX1 and either GFP-rab5Q79L (A,B) or EGF receptor GFP (C,D), then fixed 48 hours post-transfection and visualized by epifluorescence microscopy using filter sets specific for GFP (A,C) and CFP (B,D). (A,B) There is substantial overlap between rab5:Q79L (A) and CFP-SNX1 (B), especially in the enlarged endosomes. The insets above A and B are enlargements of the boxed regions and show that rab5:Q79L does not bind to GFP-SNX1 positive tubules. (C,D) There is substantial overlap between GFP-EGF receptor within cells (C) and CFP-SNX1 (D). The inserts above the panels are enlargements that reveal the presence of some EGF receptor-GFP (black arrowheads) in CFP-SNX1-positive tubules (white arrowheads). N marks the position of the nucleus in each cell. Compared to previous images from fixed cells (Fig. 5), better preservation of tubules was accomplished by fixation in 0.9% paraformaldehyde. Scale bars, 10 μm.

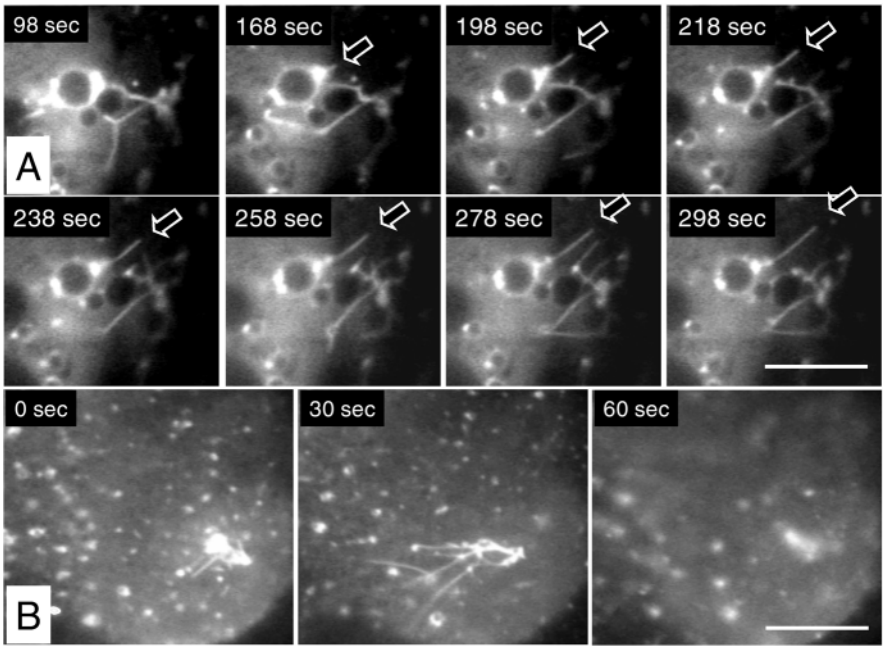

Fig. 7. Membrane tubules bud from GFP-SNX1-coated endosomes. (A) GFP-SNX1 expressing CV1 cells were examined under reduced illumination by epifluorescence microscopy and time-lapse images were captured with a frame grabber. A region containing a budding event was identified and extracted from an 8 minute movie (see movie 1, http://www.biologists.com/JCS/movies/jcs2058.html). The elapsed times are indicated in the upper left corner of each frame. Scale bar, 10 μm. The arrow marks a budding tubule as it grew over the course of 130 seconds. Also present are other tubules and vesicles. Note that all of the larger vesicles appear to have smaller vesicles docked to them. (B) Frames depicting a transient endosomal structure were extracted from an 8 minute movie (movie 2). In this sequence, we observed the enlargement of a GFP-SNX1 labeled endosome structure and its rapid diminution by GFP-SNX1 tubules moving toward the center of the cell. Scale bar, 10 μm.

more than one type of complex. Indeed, an additional endosomal protein, Hrs, has recently been found to exist in a complex with SNX1 and to participate in ligand-dependent EGF receptor downregulation (Chin et al., 2000). Interestingly, the consequence of Hrs overexpression is an inhibition of EGF receptor downregulation that is correlated with the formation of an SNX1- and Hrs-containing complex that excludes EGF receptors. Thus, Hrs appears to act as a negative regulator of the SNX1 complex.

Equilibrium between soluble and membrane-bound pools of SNX1

By analogy to the retromer complex, the SNX1 complexes probably provide a coat function. The uniform (as opposed to discontinuous) labeling of vesicles and tubules by GFP-SNX1 is consistent with this hypothesis. However, this coat appears to be somewhat labile because cell disruption in low ionic strength buffer resulted in a shift of SNX1 from membranes to cytosol in several cell lines. To determine if this reflected a dynamic equilibrium between membrane and cytosolic SNX1 in vivo, we used laser photobleaching to destroy the fluorescence of GFP-SNX1 on selected vesicles and then monitored the recovery of fluorescence. Laser pulses were attenuated such that only the fluorophore, and not the proteins themselves, were denatured. We observed a rapid recovery of cytoplasmic fluorescence followed by a slower recovery of

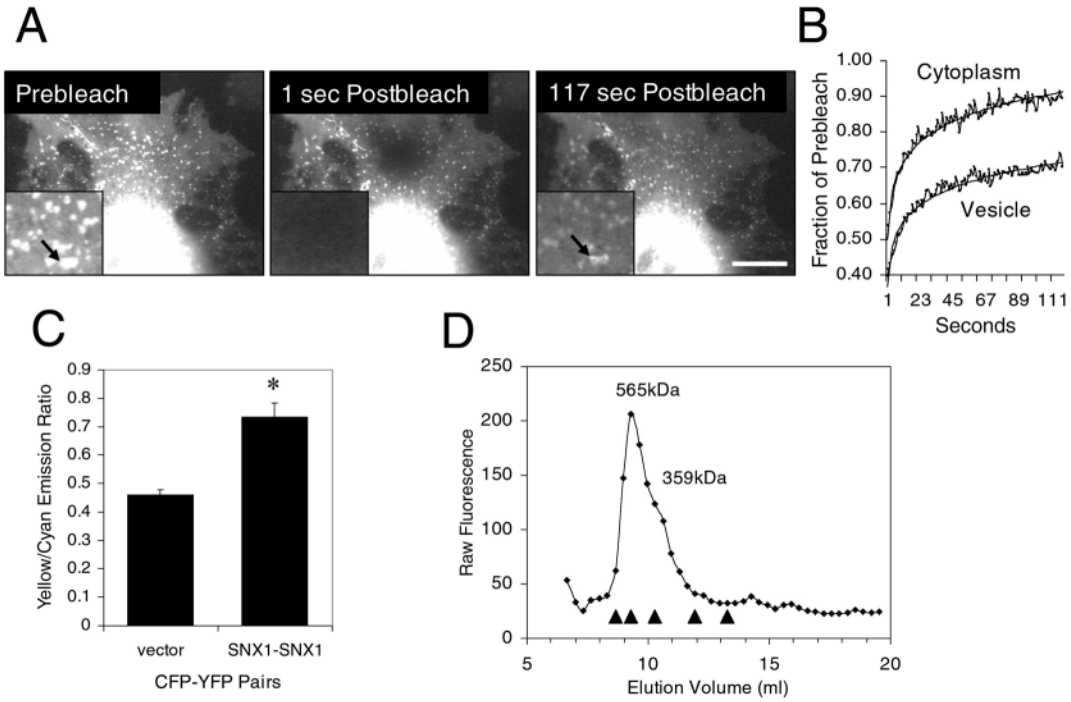

Fig. 8. GFP-SNX1 complexes bind reversibly to endosomes. (A) A relatively static region within a GFP-SNX1 transfected cell was photobleached using a dye laser (movie 3). Scale bar, 20 μm. Fluorescence intensity was measured from digital images collected at 1-second intervals for specific vesicles within the bleached zone and compared to fluorescence intensity in the adjacent cytoplasm. (B) Fluorescence recovery curves for vesicles and adjacent cytoplasm were fit to inverse exponential functions and half times for recovery of fluorescence were calculated. For five vesicles within the bleached zone in this cell, the half time for recovery in the vesicles was 14.0±0.6 seconds and the half-time for recovery in the cytoplasm was 10.5±0.5 seconds. The arrow in the inset of the bleached zone in A indicates the endosome from which the plot was derived. (C) Complex formation by SNX1 in vivo was evaluated by fluorescence resonance energy transfer. CV1 cells were cotransfected with equimolar amounts of cDNAs encoding CFP and YFP (vector) or CFP-SNX1 and YFP-SNX1. After 48 hours, cells were analyzed for fluorescence resonance energy transfer from CFP to YFP. Spatially averaged emission ratios from 9 or 10 cells for each FRET pair are plotted. The emission ratio from the CFP/YFP pair represents the baseline in the assay and is due to spectral overlap between CFP and YFP emissions. There was a statistically significant increase in the FRET ratio in CFP-SNX1/YFP-SNX1 transfected cells compared to CFP/YFP controls. The plot is representative of four experiments that showed a 44±14% increase in the FRET ratio for CFP-SNX1/YFP-SNX1. (D) GFP-SNX1 was tetrameric in HEK293 cytosols chromatographed on a Superdex 200 column. The calculated mass of proteins in the middle and shoulder of the peak correspond to hexamers and tetramers of GFP-SNX1 (89.2 kDa), respectively. The triangles, from left to right, indicate the predicted elution positions for octamers, hexamers, tetramers, dimers and monomers of GFP-SNX1. Based on the behavior of bacterial and epitope-tagged SNX1, we suggest that the 565 kDa peak represents a complex between SNX1 tetramers and other cytosolic proteins.

vesicular fluorescence that was complete within a minute of the bleaching pulse. Because the pre-bleach GFP-SNX1 was not destroyed, and labeled GFP-SNX1 vesicles do not increase in intensity over time, we conclude that steady-state labeling of vesicles with GFP-SNX1 reflects equilibrium between SNX1 association and dissociation from membranes. Rapid dissociation of SNX1 complexes from membranes could provide for plasticity in the vesicular compartment labeled by SNX1. In particular, reversibility may be an important mechanism enabling the formation of transient sorting complexes. Indeed, the tubulovesicular structures we observe with GFP-SNX1 do appear to be transient. This property could be specific for sorting by endosomal retention (French et al., 1994), given that rapid exchange of subunits has not been documented for other coat proteins.

Our biochemical experiments indicate that a fundamental unit of exchange in a SNX1 complex is a tetramer. Alternatively, the tetramer could represent a storage pool that provides homo-dimers for exchange between different types of complexes. Potential interaction sites for other proteins in the complex include the PX domain (Ponting, 1996) and the carboxyl terminus that interacts with EGF receptor (Kurten et al., 1996) and Hrs (Chin et al., 2000). In this regard, numerous cDNAs encoding SNX-related proteins have been identified. With the exception of SNX2 (61% identical to SNX1), the highest sequence conservation between these SNX1 related proteins is in the PX domain. Thus, the PX domain represents a prime candidate for interaction with additional proteins in the SNX1 complex, one of which is likely to be SNX2 (Haft et al., 1998).

Flux through the compartment defined by GFP-SNX1

GFP-SNX1 labels an endocytic compartment, as judged by accessibility to Texas Red-dextran. The GFP-SNX1 compartment shares substantial overlap with EEA1, an early endosome marker, but much less with the trans-Golgi network marker TGN 38 and the late endosome and lysosomal marker LAMP1. In addition, CFP-SNX1 colocalized to GFP-rab5:Q79L enlarged endosomes. Thus, there is overlap but not identity between the GFP-SNX1 labeled compartment and the

early endosome. The GFP-SNX1 compartment is also largely distinct from the recycling endosome, as judged by Texas Red-transferrin uptake. Due to low levels of EGF receptor expression, we could not reliably document transit of Texas Red-EGF into or through the GFP-SNX1 compartment. However, in cells cultured in serum (and hence engaged in steady-state trafficking of EGF receptors), we do detect EGF receptor-GFP and CFP-SNX1 in the same vesicles. In addition, and by contrast to every other marker used in this study, we find that EGF receptors labeled with GFP are detectable in the tubules emanating from these vesicles. Because the movement of these tubules is vectorial, the presence of EGF receptors may indicate that they are being preferentially sorted out of the large SNX1 labeled vesicles. Alternatively, these tubules could also represent the earliest stages of recycling tubules via which EGF receptors are being returned to the cell surface. However, if this were the case, then we should have been able to colocalize Texas Red-transferrin and transferrin receptors in these tubules.

We have measured GFP-SNX1 labeled vesicles as large as 6 μm in diameter. These large vesicles could be a consequence of overexpressing SNX1, as is the case for wild-type or GTPase-defective mutants of rab5 like rab5:Q79L (Stenmark et al., 1994). However, large vesicles are detectable in cells expressing differing levels of SNX1 and they are labeled to different extents themselves in a single cell. Furthermore, we observed budding of tubules that reduced the diameter and even largely abolished the parent endosome. Thus, GFP-SNX1 binding to membranes does not appear to directly induce the formation of enlarged endosomes. Rather, the vesicular structures labeled by GFP-SNX1 may represent precursors and/or remnants of transient sorting endosomes into which early endosomes deliver material and from which tubules remove material. We also noted the extensive docking of smaller vesicles with larger ones and that these docked complexes were long-lived and detected on most large endosomes. Taken together, the compartment marker and time-lapse studies indicate that GFP-SNX1 labels a transient compartment with properties common to sorting endosomes. In particular, the tubulovesicular geometry is proposed to provide a mechanism for physical sorting in the sorting endosome (Mukherjee et al., 1997). Importantly, tubule budding from GFP-SNX1 endosomes is vectorial, in that the direction of membrane flow is out of the endosome. In general, the loss of membrane by budding appears to exceed the rate of delivery of membrane by vesicles, thereby making these organelles transient structures. Indeed, in our time-lapse studies we have observed one instance of a transient vesicle, which appears and from which tubules emanate, thereby eliminating the vesicle. Thus, we suggest that the SNX1 labeled tubulovesicular compartment is a sorting endosome. These endosomes are largely distinct from recycling endosomes and overlap substantially, though not completely, with the early endosomal compartment.

Our current findings indicate that SNX1 binds as a complex to the sorting endosome, coating the membrane with protein. The precise role of SNX complexes remains to be defined: self-assembly is indicative of a structural role, yet receptor specificity is indicative of a role in selectivity. Perhaps distinct domains in SNX1 subserve both functions. A working hypothesis is that the binding of specific receptors to SNX1-coated membranes contributes to a retention step in sorting. We propose that the reversible binding of SNX1 to endosomal membranes provides for vectorial flow of membrane through the sorting compartment. In this model, SNX1 associates with incoming early endosomes as they fuse with the sorting endosome. Consequently, sorting endosomes are also positive for the early endosome marker EEA1. SNX1 remains associated with sorting endosome tubules budding from the sorting endosome, but early endosome markers do not. With time, SNX1 also dissociates from these tubules into a cytoplasmic pool capable of reassociating with early endosome and sorting endosome membranes. An important test of this model will be to determine if transferrin receptors are present in the sorting endosome tubules that contain EGF receptors. If so, then we would suggest that GFP-SNX1 labeled tubules represent the earliest phases of the recycling compartment. Alternatively, if the sorting endosome tubules lack transferrin receptors, then they should represent the earliest phases of the late endosome compartment. Studies are in progress to distinguish between these two possibilities, and immunoelectron microscopy studies indicate that the correct prediction is the latter (Gill et al., 2000).

SNX1 may have a more general function in membrane trafficking than that originally inferred based on its binding to EGF receptors. For example, the large size and the accessibility of some GFP-SNX1 vesicles to Texas Red-dextran might also indicate a role for pinocytic vesicle processing. Likewise, other mechanisms are also clearly involved in EGF receptor degradation. For example, a diluecine motif (^{679}LL) distinct from the SNX1 binding site (^{954}YLVI) on the EGF receptor has been shown to be obligatory for EGF receptor degradation (Kil et al., 1999) and could have its own signal recognition protein. In addition, C-cbl plays an important role in EGF receptor ubiquination and proteolysis that is mediated by a phosphorylated EGF receptor tyrosine residue (^{1045}Y) (Levkowitz et al., 1999). It will be important to determine if these processes are part of an overall mechanism or if they represent distinct and redundant processes that ensure rapid receptor downregulation. GFP fusion proteins will provide useful molecular markers with which to further dissect the sorting endosome compartment and the process of EGF receptor sorting in living cells. In combination with biochemical approaches, direct visualization of trafficking proteins and receptors provides a valuable tool for understanding the molecular heterogeneity with respect to the types of complexes formed by SNX1 and the apparent mechanistic heterogeneity of EGF receptor trafficking.

We are grateful to Gordon N. Gill, University of California, San Diego, USA for providing the HeLa cells expressing HA-SNX1; Alexander Sorkin, University of Colorado Health Science Center for providing the EGF receptor GFP plasmid; Philip Stahl, Washington University School of Medicine, for providing the GFP rab5 plasmids; Margaret McIntire and Christian Eyiuche for technical support. Monoclonal antibodies H4A3 against LAMP-1 and H4B4 against LAMP-2 developed by J. T. August and J. E. K. Hildreth were obtained from the Developmental Studies Hybridoma Bank developed under the auspices of the NICHD and maintained by The University of Iowa, Department of Biological Sciences, Iowa City, IA 52242, USA. This work was supported by ACS RPG 97-102-01-C.S.M. to R.C.K.

REFERENCES

Aoe, T., Lee, A. J., van Donselaar, E., Peters, P. J. and Hsu, V. W. (1998). Modulation of intracellular transport by transported proteins: insight from regulation of COPI-mediated transport. *Proc. Natl. Acad. Sci. USA* **95**, 1624-1629.

Aridor, M., Weissman, J., Bannykh, S., Nuoffer, C. and Balch, W. E. (1998). Cargo selection by the COPII budding machinery during export from the ER. *J. Cell Biol.* **141**, 61-70.

Berdichevsky, F., Alford, D., D'Souza, B. and Taylor-Papadimitriou, J. (1994). Branching morphogenesis of human mammary epithelial cells in collagen gels. *J. Cell Sci.* **107**, 3557-3568.

Cadena, D. L., Chan, C. L. and Gill, G. N. (1994). The intracellular tyrosine kinase domain of the epidermal growth factor receptor undergoes a conformational change upon autophosphorylation. *J. Biol. Chem.* **269**, 260-265.

Candido, E. P., Reeves, R. and Davie, J. R. (1978). Sodium butyrate inhibits histone deacetylation in cultured cells. *Cell* **14**, 105-113.

Carter, R. E. and Sorkin, A. (1998). Endocytosis of functional epidermal growth factor receptor-green fluorescent protein chimera. *J. Biol. Chem.* **273**, 35000-35007.

Chalfie, M., Tu, Y., Euskirchen, G., Ward, W. W. and Prasher, D. C. (1994). Green fluorescent protein as a marker for gene expression. *Science* **263**, 802-805.

Chang, C. P., Lazar, C. S., Walsh, B. J., Komuro, M., Collawn, J. F., Kuhn, L. A., Tainer, J. A., Trowbridge, I. S., Farquhar, M. G., Rosenfeld, M. G. et al. (1993). Ligand-induced internalization of the epidermal growth factor receptor is mediated by multiple endocytic codes analogous to the tyrosine motif found in constitutively internalized receptors. *J. Biol. Chem.* **268**, 19312-19320.

Chen, J. W., Murphy, T. L., Willingham, M. C., Pastan, I. and August, J. T. (1985). Identification of two lysosomal membrane glycoproteins. *J. Cell Biol*. **101**, 85-95.

Chin, L. S., Raynor, M. C., Wei, X., Chen, H. Q. and Li, L. (2000). Hrs interacts with sorting Nexin 1 and regulates degradation of epidermal growth factor receptor. *J. Biol. Chem*. **276**, 7069-7078.

Dautry-Varsat, A., Ciechanover, A. and Lodish, H. F. (1983). pH and the recycling of transferrin during receptor-mediated endocytosis. *Proc. Natl. Acad. Sci. USA* **80**, 2258-2262.

Davis, C. G., Goldstein, J. L., Sudhof, T. C., Anderson, R. G., Russell, D. W. and Brown, M. S. (1987). Acid-dependent ligand dissociation and recycling of LDL receptor mediated by growth factor homology region. *Nature* **326**, 760-765.

Dunn, K. W., McGraw, T. E. and Maxfield, F. R. (1989). Iterative fractionation of recycling receptors from lysosomally destined ligands in an early sorting endosome. *J. Cell Biol.* **109**, 3303-3314.

Faundez, V., Horng, J. T. and Kelly, R. B. (1998). A function for the AP3 coat complex in synaptic vesicle formation from endosomes. *Cell* **93**, 423-432.

Felder, S., Miller, K., Moehren, G., Ullrich, A., Schlessinger, J. and Hopkins, C. R. (1990). Kinase activity controls the sorting of the epidermal growth factor receptor within the multivesicular body. *Cell* **61**, 623-634.

French, A. R., Sudlow, G. P., Wiley, H. S. and Lauffenburger, D. A. (1994). Postendocytic trafficking of epidermal growth factor-receptor complexes is mediated through saturable and specific endosomal interactions. *J. Biol. Chem.* **269**, 15749-15755.

Gill, G. N., Lazar, C. S., Yea, M., Zhong, Q. and Meerloo, T. (2000). Interactions among sorting nexins. *Mol. Biol. Cell* **11**, 214a.

Goldberg, J. (2000). Decoding of sorting signals by coatomer through a GTPase switch in the COPI coat complex. *Cell* **100**, 671-679.

Graham, F. L. and Eb, A. J. v. d. (1973). A new technique for the assay of infectivity of human adenovirus 5 DNA. *Virology* **52**, 456-467.

Guarnieri, F. G., Arterburn, L. M., Penno, M. B., Cha, Y. and August, J. T. (1993). The motif Tyr-X-X-hydrophobic residue mediates lysosomal membrane targeting of lysosome-associated membrane protein 1. *J. Biol. Chem.* **268**, 1941-1946.

Haft, C. R., de la Luz Sierra, M., Barr, V. A., Haft, D. H. and Taylor, S. I. (1998). Identification of a family of sorting nexin molecules and characterization of their association with receptors. *Mol. Cell Biol.* **18**, 7278-7287.

Haft, C. R., Sierra, M. L., Bafford, R., Lesniak, M. A., Barr, V. A. and Taylor, S. I. (2000). Human Orthologs of Yeast Vacuolar Protein Sorting Proteins Vps26, 29, and 35: Assembly into Multimeric Complexes. *Mol. Biol. Cell* **11**, 4105-4116.

Herbst, J. J., Opresko, L. K., Walsh, B. J., Lauffenburger, D. A. and Wiley, H. S. (1994). Regulation of postendocytic trafficking of the epidermal growth factor receptor through endosomal retention. *J. Biol. Chem.* **269**, 12865-12873.

Honegger, A. M., Dull, T. J., Felder, S., Van Obberghen, E., Bellot, F., Szapary, D., Schmidt, A., Ullrich, A. and Schlessinger, J. (1987). Point mutation at the ATP binding site of EGF receptor abolishes protein-tyrosine kinase activity and alters cellular routing. *Cell* **51**, 199-209.

Horazdovsky, B. F., Davies, B. A., Seaman, M. N., McLaughlin, S. A., Yoon, S. and Emr, S. D. (1997). A sorting nexin-1 homologue, Vps5p, forms a complex with Vps17p and is required for recycling the vacuolar protein-sorting receptor. *Mol. Biol. Cell* **8**, 1529-1541.

Kil, S. J., Hobert, M. and Carlin, C. (1999). A leucine-based determinant in the epidermal growth factor receptor juxtamembrane domain is required for the efficient transport of ligand-receptor complexes to lysosomes. *J. Biol. Chem.* **274**, 3141-3150.

Kornilova, E., Sorkina, T., Beguinot, L. and Sorkin, A. (1996). Lysosomal targeting of epidermal growth factor receptors via a kinase-dependent pathway is mediated by the receptor carboxyl-terminal residues 1022-1123. *J. Biol. Chem.* **271**, 30340-30346.

Kurten, R. C., Cadena, D. L. and Gill, G. N. (1996). Enhanced degradation of EGF receptors by a sorting nexin, SNX1. *Science* **272**, 1008-1010.

Levkowitz, G., Waterman, H., Ettenberg, S. A., Katz, M., Tsygankov, A. Y., Alroy, I., Lavi, S., Iwai, K., Reiss, Y., Ciechanover, A. et al. (1999). Ubiquitin ligase activity and tyrosine phosphorylation underlie suppression of growth factor signaling by c-Cbl/Sli-1. *Mol. Cell* **4**, 1029-1040.

Levkowitz, G., Waterman, H., Zamir, E., Kam, Z., Oved, S., Langdon, W. Y., Beguinot, L., Geiger, B. and Yarden, Y. (1998). c-Cbl/Sli-1 regulates endocytic sorting and ubiquitination of the epidermal growth factor receptor. *Genes Dev.* **12**, 3663-3674.

Milsted, A., Day, D. L., Pensky, J. and Cox, R. P. (1987). Phenotypes of HeLa S3 variant cell lines resistant to growth inhibition by sodium butyrate. *In Vitro Cell Dev. Biol.* **23**, 395-402.

Miyawaki, A., Llopis, J., Heim, R., McCaffery, J. M., Adams, J. A., Ikura, M. and Tsien, R. Y. (1997). Fluorescent indicators for Ca^{2+} based on green fluorescent proteins and calmodulin. *Nature* **388**, 882-887.

Mukherjee, S., Ghosh, R. N. and Maxfield, F. R. (1997). Endocytosis. *Physiol. Rev.* **77**, 759-803.

Nesterov, A., Kurten, R. C. and Gill, G. N. (1995a). Association of epidermal growth factor receptors with coated pit adaptins via a tyrosine phosphorylation-regulated mechanism. *J. Biol. Chem.* **270**, 6320-6327.

Nesterov, A., Wiley, H. S. and Gill, G. N. (1995b). Ligand-induced endocytosis of epidermal growth factor receptors that are defective in binding adaptor proteins. *Proc. Natl. Acad. Sci. USA* **92**, 8719-8723.

Nothwehr, S. F. and Hindes, A. E. (1997). The yeast VPS5/GRD2 gene encodes a sorting nexin-1-like protein required for localizing membrane proteins to the late Golgi. *J. Cell Sci.* **110**, 1063-1072.

Ohno, H., Stewart, J., Fournier, M. C., Bosshart, H., Rhee, I., Miyatake, S., Saito, T., Gallusser, A., Kirchhausen, T. and Bonifacino, J. S. (1995). Interaction of tyrosine-based sorting signals with clathrin-associated proteins. *Science* **269**, 1872-1875.

Opresko, L. K., Chang, C. P., Will, B. H., Burke, P. M., Gill, G. N. and Wiley, H. S. (1995). Endocytosis and lysosomal targeting of epidermal growth factor receptors are mediated by distinct sequences independent of the tyrosine kinase domain. *J. Biol. Chem.* **270**, 4325-4333.

Pollok, B. A. and Heim, R. (1999). Using GFP in FRET-based applications. *Trends Cell Biol.* **9**, 57-60.

Ponting, C. P. (1996). Novel domains in NADPH oxidase subunits, sorting nexins, and PtdIns 3-kinases: binding partners of SH3 domains? *Protein Sci.* **5**, 2353-2357.

Presley, J. F., Cole, N. B., Schroer, T. A., Hirschberg, K., Zaal, K. J. and Lippincott-Schwartz, J. (1997). ER-to-Golgi transport visualized in living cells. *Nature* **389**, 81-85.

Roberts, R. L., Barbieri, M. A., Pryse, K. M., Chua, M., Morisaki, J. H. and Stahl, P. D. (1999). Endosome fusion in living cells overexpressing GFP-rab5. *J. Cell Sci.* **112**, 3667-3675.

Sealy, L. and Chalkley, R. (1978). The effect of sodium butyrate on histone modification. *Cell* **14**, 115-121.

Seaman, M. N., McCaffery, J. M. and Emr, S. D. (1998). A membrane coat complex essential for endosome-to-Golgi retrograde transport in yeast. *J. Cell Biol.* **142**, 665-681.

Slaaby, R., Jensen, T., Hansen, H. S., Frohman, M. A. and Seedorf, K. (1998). PLD2 complexes with the EGF receptor and undergoes tyrosine

phosphorylation at a single site upon agonist stimulation. *J. Biol. Chem.* **273**, 33722-33727.

Sorkin, A. and Carpenter, G. (1993). Interaction of activated EGF receptors with coated pit adaptins. *Science* **261**, 612-615.

Sorkin, A., Mazzotti, M., Sorkina, T., Scotto, L. and Beguinot, L. (1996). Epidermal growth factor receptor interaction with clathrin adaptors is mediated by the Tyr974-containing internalization motif. *J. Biol. Chem.* **271**, 13377-13384.

Stenmark, H., Parton, R. G., Steele-Mortimer, O., Lutcke, A., Gruenberg, J. and Zerial, M. (1994). Inhibition of rab5 GTPase activity stimulates membrane fusion in endocytosis. *EMBO J.* **13**, 1287-1296.

Vieira, A. V., Lamaze, C. and Schmid, S. L. (1996). Control of EGF receptor signaling by clathrin-mediated endocytosis. *Science* **274**, 2086-2089.

Wells, A., Welsh, J. B., Lazar, C. S., Wiley, H. S., Gill, G. N. and Rosenfeld, M. G. (1990). Ligand-induced transformation by a noninternalizing epidermal growth factor receptor. *Science* **247**, 962-964.

Wu, P. and Brand, L. (1994). Resonance energy transfer: methods and applications. *Anal. Biochem.* **218**, 1-13.

Yang, T. T., Sinai, P., Green, G., Kitts, P. A., Chen, Y. T., Lybarger, L., Chervenak, R., Patterson, G. H., Piston, D. W. and Kain, S. R. (1998). Improved fluorescence and dual color detection with enhanced blue and green variants of the green fluorescent protein. *J. Biol. Chem.* **273**, 8212-8216.